

Effect of watershed subdivision on prediction accuracy of hydrologic models

T.V. HROMADKA II

Director of Water Resources Engineering, Williamson and Schmid, Irvine, California 92714, USA

R.H. McCUEN

Professor of Civil Engineering, University of Maryland, College Park, Maryland 20742, USA

C.C. YEN

Hydrologist, Williamson and Schmid, Irvine, California 92714, USA

While much has been written about hydrologic modeling and the successes and failures of models, little detail has been paid to a key practice in watershed runoff hydrologic models – discretization. Due to the sparse rainfall-runoff data typically available at a watershed, it may be questionable whether the subdivision of the catchment into subareas which are linked together by routing elements, when there is no data to reconstitute subarea hydrologic parameters, is a “better” approach to modeling the catchment response. In this paper, the subject of catchment discretization is examined in detail. It is noted that for a linear hydrologic model based on unit hydrographs (for various levels of discretization into subareas) and translation for channel routing, a discretized model is equivalent to a simple one-subarea model, and this simple model includes the variation of effective rainfall over the watershed which is not included in the discretized model.

INTRODUCTION

The typical procedure for using a unit hydrograph (UH) type model such as TR-20 and HEC-1 is to subdivide a watershed into subareas which are linked together by channel or detention basin routing. Parameters are then assigned to the several UH subarea submodels (e.g., losses, timing, etc.) and the routing models. Oftentimes, even though the catchment may be essentially homogeneous, it will also be discretized into several subareas which are in turn linked together by routing elements. For example, it is not uncommon for a nearly homogeneous (almost uniform development, drainage patterns, etc.) 1 or 2 square mile catchment to be subdivided into one or two dozen (or more) subareas.

The questions arise as to whether (1) such subdivision practices result in “better” models; and (2) are such highly discretized models “better” for use in design purposes than simpler models based on a minimum number of subareas? In this paper the UH modeling approach is examined as to the above considerations.

First, a single area model (the “simple” model) based upon a UH, a time parameter (lag), and a simple loss function based upon a coupled fixed fraction loss (\bar{Y}) and a ϕ -index (Fm) is developed for a catchment. The simple model is then calibrated to rainfall-runoff data in order to develop optimized values for the unit hydrograph (“S” graph form), timing (lag), and the loss parameters, i.e., Fm and \bar{Y} for each reconstitution analysis. Because each storm considered resulted in different optimized parameters, a frequency-distribution is determined for the model parameters.

The next part of this study is to discretize the watershed into several subarea schematics linked together by channel routing elements. Three levels of discretization (“complex” models) are considered; namely, a 3-, 9-, and

18- subarea model. Each subarea, is assumed to be described by the same UH model as used in the simple model; that is, the S -graph (as a function of lag), Fm and \bar{Y} are assumed to take on values contained in the range of values developed from the simple model reconstitution studies. (Details of model parameters are contained in a subsequent section of this paper.)

The third part of this paper considers the model output of peak flow rate (Q) for each of the several models considered. More specifically, the variance of the peak flow rate or $\text{Var}(Q)$ as a result of parameter uncertainty is examined for each of the complex models and also the simple model. Several variations on this theme are considered; such as the effects of homogeneity and non-homogeneity on loss rates in a complex model, the $\text{Var}(Q)$ due to channel routing parameter uncertainty, and the $\text{Var}(Q)$ due to storm magnitude (e.g., 100-year versus 10-year design storms). An estimator giving a bound on the $\text{Var}(Q)$ is developed. It is shown that, usually, $\text{Var}(Q)$ decreases as the number of subareas increase.

Addressed in this study is the issue that, in general, a single stream gauge and a single rain gauge is used to calibrate the simple UH model. For each storm reconstituted, optimized parameters are obtained which best “correlate” the rain gauge and stream gauge data. This is only a “correlation” because the available rain gauge data oftentimes provides only a gross estimate of the actual rainfall distributions over the entire watershed. As more storms are analyzed and “best fit” model parameters are developed, a set of values are obtained for each model parameter set which can be arranged into a frequency-distribution. This frequency-distribution or parameter sets displays the statistical correlation between the available rainfall-runoff data, and the assumed model. Consequently,

the $Var(Q)$ due to the variation in the model optimized parameter sets reflects the variation in the correlation between the available rainfall-runoff data.

However for the discretized ("complex") model, the $Var(Q)$ decreases (typically) as the number of subareas increase where now the $Var(Q)$ represents the variance in the complex model peak flow rate as the optimized model parameter sets vary independently in each subarea. But obviously the knowledge of the effective rainfall distribution over the watershed does not increase due to an increased model complexity by adding more subareas. Rather, the decrease in the $Var(Q)$ for a complex model reflects a departure of the modeling results from the true catchment hydrologic behavior.

1. RUNOFF HYDROGRAPH MODEL

The unit hydrograph (UH) model is based upon several parameters; namely, two loss rate parameters (a phi index coupled with a fixed percentage), an S -graph, and catchment lag.

Loss function

The loss function, $f(t)$, used in the model is defined by

$$f(t) = \begin{cases} \bar{Y}I(t), & \text{for } \bar{Y}I(t) < F_m \\ F_m, & \text{otherwise} \end{cases} \quad (1)$$

where \bar{Y} is the low loss fraction, $I(t)$ is rainfall intensity at time t , and F_m is a maximum loss rate.

Figure 1 illustrates the considered loss rate function. The use of a constant percentage loss rate \bar{Y} in Eq. 1 is reported in Scully and Bender (1969)¹. The use of a phi (ϕ -index) method in effective rainfall calculations is also well-known (e.g., Kibler)².

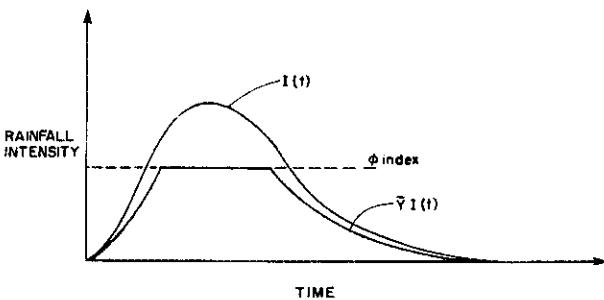


Figure 1. Soil-loss function

For a given storm, the low loss fraction is determined by

$$\bar{Y} = 1 - Y \quad (2)$$

where Y is the ratio of (total measured effective rainfall)/(total measured runoff).

From the above relationships, the low loss fraction, \bar{Y} , acts as a fixed loss rate percentage, whereas F_m serves as an upper bound to the possible values of $f(t) = \bar{Y}I(t)$. Values for F_m are developed from the rainfall-runoff reconstitution studies of several significant storm events for the watershed under study.

S -graph

The S -graph representation of the unit hydrograph (e.g., McCuen and Bondelid, 1983³; Chow and Kulandalswamy,

1982⁴; Mays and Coles, 1980⁵) can be used to develop unit hydrographs corresponding to various watershed lag estimates. The S -graph is developed by rainfall-runoff reconstitution studies of several storms. Because the loss parameter Y is readily determined in Eq. (2), the S -graph and F_m parameters are determined for each storm considered by trial-and-error until an optimum fit is developed between the model produced runoff hydrograph and measured runoff hydrograph (i.e., a reconstitution analysis).

Lag

Fundamental to any hydrologic model is a catchment timing parameter. The watershed lag is defined as the time from the beginning of effective rainfall to that time corresponding to 50-percent of the S -graph ultimate discharge. Catchment lag is estimated directly from the S -graph reconstituted from each storm considered.

Runoff hydrograph model

The UH model results in a time distribution of runoff $Q(t)$ given by the standard convolution integral representation of

$$Q(t) = \int_0^t e(t-s) u(s) ds \quad (3)$$

where $Q(t)$ is the catchment flow rate at the point of concentration; $e(t-s)$ is the effective rainfall intensity; and $u(s)$ is the unit hydrograph developed from the particular S -graph.

Optimized parameter sets and model uncertainty analysis

In a reconstitution study, the "best fit" between the model runoff hydrograph $Q(t)$ and the measured (stream gauge) runoff hydrograph is determined by trial-and-error. Typically, \bar{Y} was estimated by Eq. (2) and this estimate was used in fitting while the S -graph and F_m parameters were optimized, and then \bar{Y} was varied and the cycle repeated, if needed.

Consequently, each storm has an associated set of parameters, those for the i -th storm being represented by the vector P_i ; which correlate (by the model) the available rainfall and runoff data. A different storm would have another optimum parameter set. Indeed, it is possible for the available rain gauge data to indicate nearly identical storm events and yet the measured runoff hydrographs to be so dissimilar that the two sets of "best-fit" parameters are quite different.

Ideally, hundreds of significant storm events would be available for the study watershed so that hundreds of optimized parameter sets could be determined. Then, the universe spanned by these parameter sets could be analyzed in order to develop a frequency-distribution for the parameter sets. Then for design purposes, the variation in the design output can be analyzed by evaluating the entire universe of parameter sets. However due to limited data, only a few storms are available for developing the optimized parameter sets and additional data is required in order to analyze the model uncertainty.

To supplement the available data, additional information can be obtained from neighboring watersheds, considered "hydrologically" similar. Thus, several watersheds are grouped together in order to obtain a larger

population of optimized parameter sets. But when even several watersheds considered together, the universe of optimum parameter sets is still small.

Another consumption which can be used to facilitate the model uncertainty analysis is to assume the individual parameters (e.g., the S -graph and loss rate parameters) to be statistically independent. That is, each optimum parameter set is composed of individual parameter values which have their own respective frequency-distributions, and the probability of occurrence of a particular optimum parameter set is equal to the product of the several parameter probability of occurrences. In this fashion, the universe of possible "optimum" parameter sets grows enormously, and a model uncertainty analysis becomes more tractable.

It is noted that although the model uncertainty analysis is a key concern, this study focuses more on the differences in decision making resulting from the use of simpler UH models using a few subareas as compared to UH models using a highly discretized subarea schematic. Consequently, it is assumed that the conclusions drawn between use of the two levels of model discretization by use of the expanding universe of parameter sets are similar to the conclusions drawn by use of a frequency-distribution of optimized parameter sets, had this frequency distribution been of sufficient sample size.

Rainfall-runoff data

Considerable rainfall-runoff calibration data has been prepared by the Corps of Engineers (COE) for use in their flood control design and planning studies. Much of this information has been prepared during the course of routine flood control studies in Orange County and Los Angeles County, but additional information has been compiled in preliminary form for ongoing COE studies for the massive Santa Ana River project (Los Angeles County Drainage Area, or LACDA). The watershed information available includes rainfall-runoff reconstitution studies for three or more significant storms for each watershed, developing optimized estimates for the S -graph, lag, and peak loss rate at the peak rainfall intensities. Although the COE used a more rational Horton type loss function which decreases with time, only the loss rate that occurred during the peak storm rainfalls was used in the calibration effort reported herein.

A total of 12 watersheds were considered in detail for our study. Seven of the watersheds are located in Los Angeles County while the other five catchments are in Orange County (Figure 2). Several other local watersheds were also considered in light of previous COE studies that resulted in additional estimates of loss rates, S -graphs, and lag values. Table 1 provides an itemization of data obtained from the COE studies, and watershed data assumed for catchments considered hydrologically similar to the COE study catchments.

Peak loss rate, F_p

From Table 1, several peak rainfall loss rates are tabulated which include, when appropriate, two loss rates for double-peak storms. The range of values for all F_p estimates lie between 0.30 and 0.65 inch/hour with the highest value occurring in Verdugo Wash which has substantial open space in foothill areas. Except for Verdugo Wash, $0.20 \leq F_p \leq 0.60$ which is a variation in values of the order noted for Alhambra Wash alone. Figure 3 shows a histogram of F_p values for the several watersheds. It is evident from the figures

that 88 percent of F_p values are between 0.20 and 0.45 inch/hour, with 77 percent of the values falling between 0.20 and 0.40 inch/hour. Consequently, a regional mean value of F_p equal to 0.30 inch/hour approximates nearly 80 percent of the F_p values, for all watersheds, for all storms, within 0.10 inch/hour.



Figure 2. Location of Drainage Basins

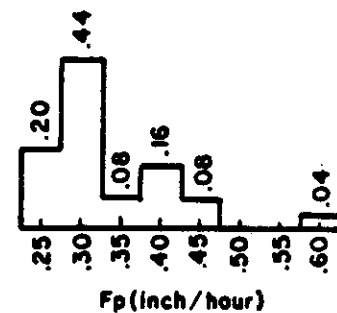


Figure 3. Frequency-distribution for F_p

S -graph

Each of the watersheds listed in Table 1 has S -graphs developed for each of the storms where peak loss rate values were developed. For example, Figure 4 shows the several S -graphs developed for Alhambra Wash. By averaging the several S -graph ordinates (developed from rainfall-runoff data), an average S -graph was obtained. By combining the several watershed average S -graphs (Figure 5) into a single plot, an average of averaged S -graphs is obtained. This regionalized S -graph (Urban S -graph in Figure 5) can be proposed as a regionalized S -graph for the several watersheds. Indeed, the variation in S -graphs for a single watershed for different storms (see Figure 4) is of the order of magnitude of variation seen between the several catchment averaged S -graphs.

In order to quantify the effects of variations in the S -graph due to variations in storms and in watersheds, the scaling of Figure 6 was used where the variable "X" signifies the average value of an arbitrary S -graph as a linear combination

Table 1. Watershed Characteristics

| Watershed Name | Watershed Geometry | | | | | Calibration Results | | | | |
|---------------------------------------|-----------------------------|-------------|-------------------------|---------------|------------------------|---------------------|-------------------------------|--------------------------------|-----------|---|
| | Area (mi ²) | Length (mi) | Length of Centroid (mi) | Slope (ft/mi) | Percent Impervious (%) | Tc (Hrs) | Storm Date | Peak F _p (inch/hr) | Lag (hrs) | Basin factor |
| Alhambra Wash ¹ | 13.67 | 8.62 | 4.17 | 82.4 | 45 | 0.89 | Feb. 78 Mar. 78 Feb. 80 | 0.59,0.24 0.35,0.29 0.24 | 0.62 | 0.015 |
| Compton 2 ¹ | 24.66 | 12.69 | 6.63 | 13.8 | 55 | 2.22 | Feb. 78 Mar. 78 Feb. 80 | 0.36 0.29 0.44 | 0.94 | 0.015 |
| Verdugo Wash ¹ | 26.8 | 10.98 | 5.49 | 316.9 | 20 | — | Feb. 78 | 0.65 | 0.64 | 0.016 |
| Limekiln ¹ | 10.3 | 7.77 | 3.41 | 295.7 | 25 | — | Feb. 78 Feb. 80 | 0.27 0.27 | 0.73 | 0.026 |
| San Jose ² | 83.4 | 23.00 | 8.5 | 60.0 | 18 | — | Feb. 78 Feb. 80 | 0.20 0.39 | 1.66 | 0.020 |
| Sepulveda ² | 152.0 | 19.0 | 9.0 | 143.0 | 24 | — | Feb. 78 Mar. 78 Feb. 80 | 0.22,0.21 0.32 0.42 | 1.12 | 0.017 |
| Eaton Wash ¹ | 11.02 ⁴ (57%) | 8.14 | 3.41 | 90.9 | 40 | 1.05 | — | — | — | 0.015 ⁷ |
| Rubio Wash ¹ | 12.20 ⁵ (3%) | 9.47 | 5.11 | 125.7 | 40 | 0.68 | — | — | — | 0.015 ⁷ |
| Arcadia Wash ¹ | 7.70 ⁶ (14%) | 5.87 | 3.03 | 156.7 | 45 | 0.60 | — | — | — | 0.015 ⁸ |
| Compton 1 ¹ | 15.08 | 9.47 | 3.79 | 14.3 | 55 | 1.92 | — | — | — | 0.015 ⁸ |
| Dominguez ¹ | 37.30 | 11.36 | 4.92 | 7.9 | 60 | 2.08 | — | — | — | 0.015 ⁸ |
| Santa Ana Delhi ³ | 17.6 | 8.71 | 4.17 | 16.0 | 40 | 1.73 | — | — | — | 0.053 ⁹ 0.040 ¹⁰ |
| Westminster ³ | 6.7 | 5.65 | 1.39 | 13 | 40 | — | — | — | — | 0.079 ⁹ 0.040 ¹⁰ |
| El Modena-Irvine ³ | 11.9 | 6.34 | 2.69 | 52 | 40 | 0.78 | — | — | — | 0.028 ⁹ |
| Garden Grove-Wintersberg ¹ | 20.8 | 11.74 | 4.73 | 10.6 | 64 | 1.98 | — | — | — | — |
| San Diego Creek ¹ | 36.8 | 14.2 | 8.52 | 95.0 | 20 | 1.39 | — | — | — | — |

Notes

- 1 : Watershed Geometry based on review of quadrangle maps and LACFCD storm drain maps.
- 2 : Watershed Geometry based on COE LACDA Study.
- 3 : Watershed Geometry based on COE Reconstitution Study for Santa Ana Delhi and Westminster Channels (June, 1983).
- 4 : Area reduced 57% due to several debris basins and Eaton Wash Dam reservoir, and groundwater recharge ponds.
- 5 : Area reduced 3% due to debris basin.
- 6 : Area reduced 14% due to several debris basins.
- 7 : 0.013 basin factor reported by COE (subarea characteristics, June, 1984).
- 8 : 0.015 basin factor assumed due to similar watershed values of 0.015.
- 9 : Average basin factor computed from reconstitution studies.
- 10 : COE recommended basin factor for flood flows.

of the steepest and flattest S-graphs obtained. That is, all the S-graphs (all storms, all catchments) lie between the Feb. 1978 storm Alhambra S-graph (X = 1) and the San Jose S-graph (X = 0). To approximate a particular S-graph of the sample set,

$$S(X) = X S_1 + (1 - X) S_2 \tag{4}$$

where S(X) is the S-graph as a function of X, and S₁ and S₂ are the Alhambra (Feb. 1978 storm) and San Jose S-graphs,

respectively. Figure 7 shows the population distribution of X where each watershed is weighted equally in the total distribution (i.e., each watershed is represented by an equal number of X entries). Table 2 lists the X values obtained from the Figure 6 scalings of each catchment S-graph. In the table, the "upper" and "lower" X-value that corresponds to the X coordinate at 80 percent and 20 percent of ultimate discharge values, respectively, is listed.

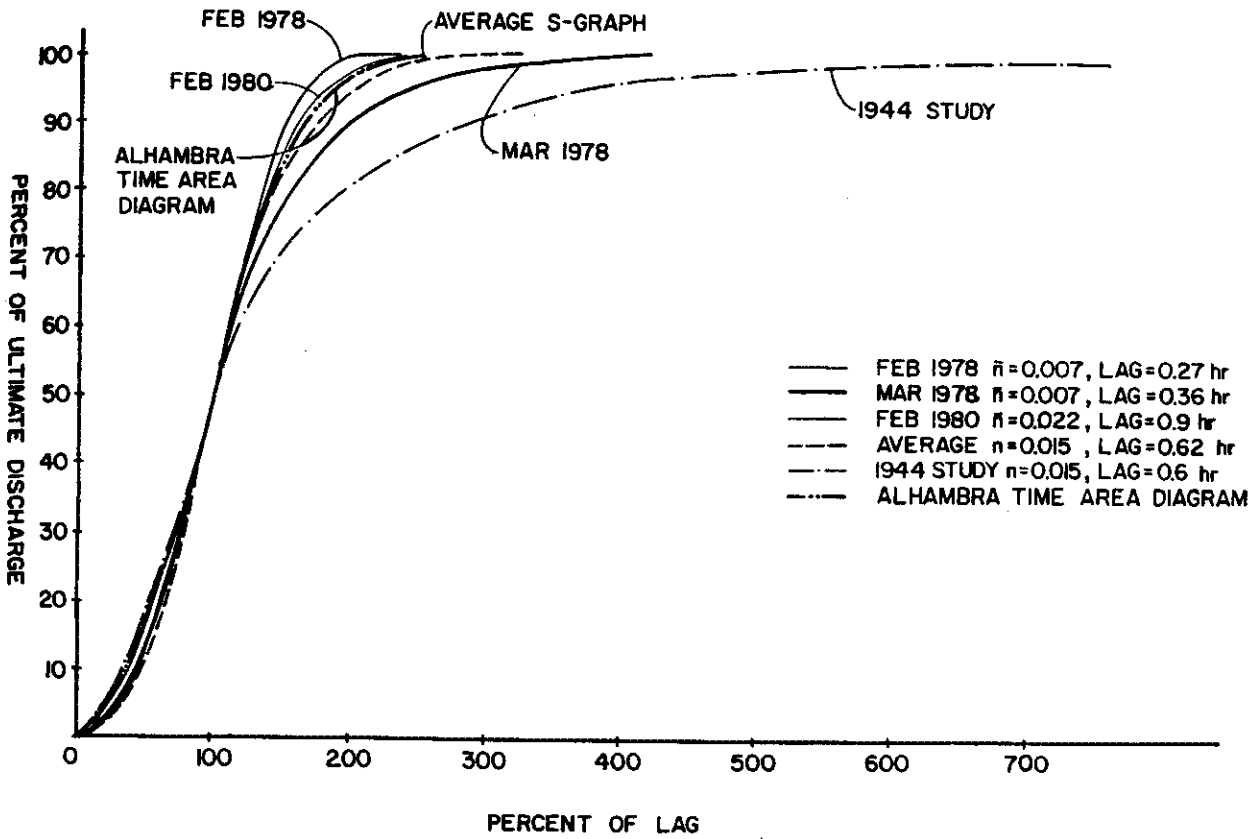


Figure 4. Alhambra Wash S-Graphs

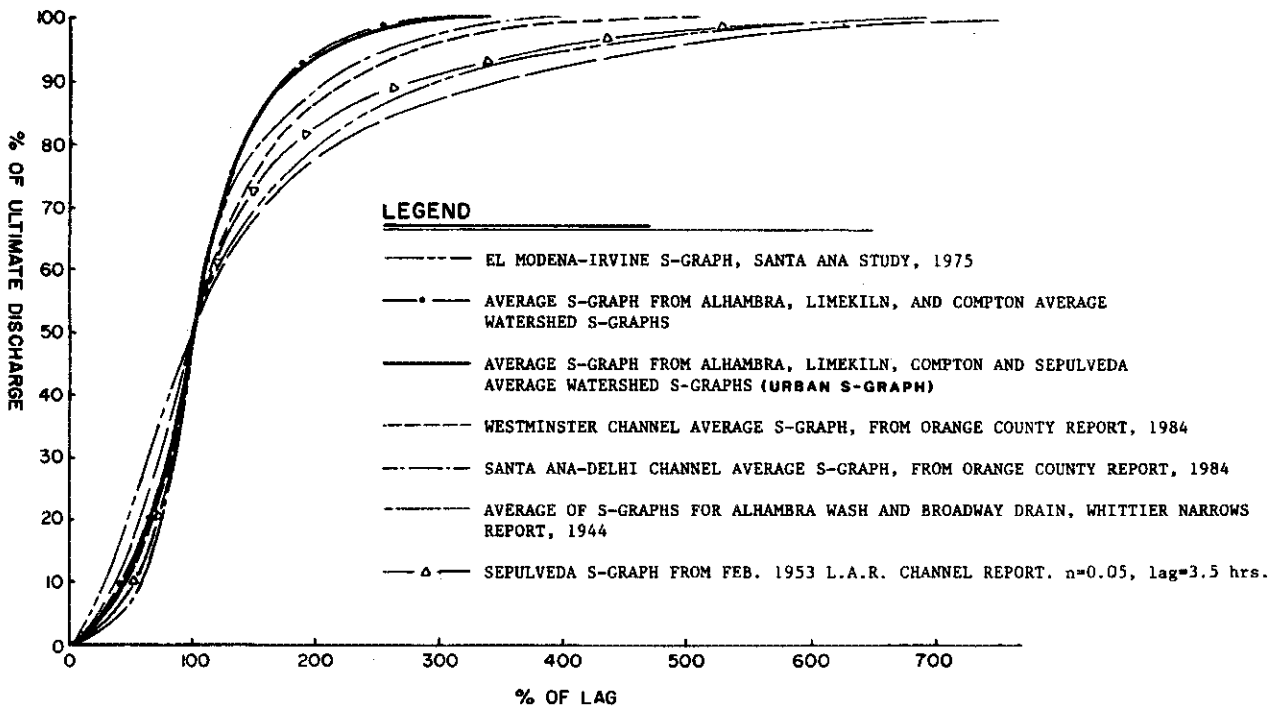


Figure 5. Average S-Graphs

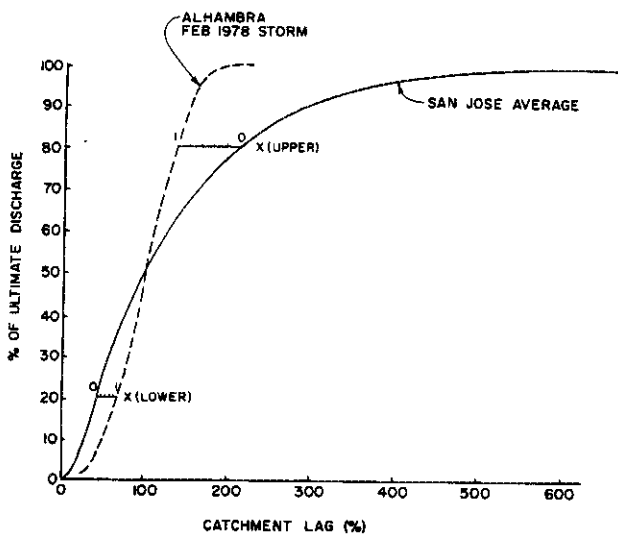


Figure 6. S-Graph Scaling for $S(X)$

Table 2. Catchment S-Graph X-Values

| Watershed Name | Storm | X (Upper) | X (Lower) | X (Avg) |
|-----------------|---------|-----------|-----------|---------|
| Alhambra | Feb. 78 | 1.00 | 1.00 | 1.00 |
| | Feb. 80 | 0.95 | .60 | 0.78 |
| | Mar. 78 | 0.70 | .80 | 0.75 |
| Limekiln | Feb. 78 | 0.50 | 0.80 | 0.65 |
| | Feb. 80 | 0.80 | 1.00 | 0.90(2) |
| Sepulveda | AVG. | 0.90 | 0.80 | 0.85(3) |
| Compton | AVG. | 0.90 | 1.00 | 0.95(3) |
| Westminster | AVG. | 0.60 | 0.60 | 0.60(3) |
| Santa Ana Delhi | AVG. | 0.80 | 1.00 | 0.90(3) |
| Urban | AVG. | 0.90 | 0.80 | 0.85 |

In Table 2, the numbers in parenthesis indicate a weighting of the average X value. That is, due to only the average S-graph (previously derived by the COE) being available, it is weighted so that all catchments are equally represented in the sample set.

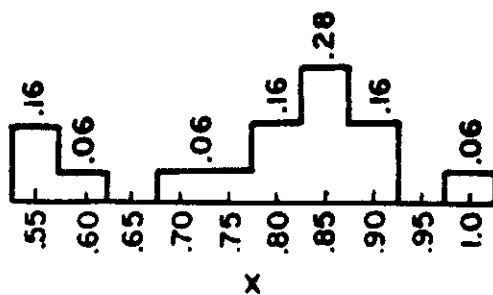


Figure 7. Frequency-Distribution for S-Graph "X"

Catchment lag

From the S-graph reconstituted for each storm, a lag value is determined by the definition. Because each storm analyzed resulted in a different optimum S-graph, the corresponding lag also varied. Based on the several storms considered for all the watersheds, the variation in lag is represented by the frequency-distribution shown in Figure 8.

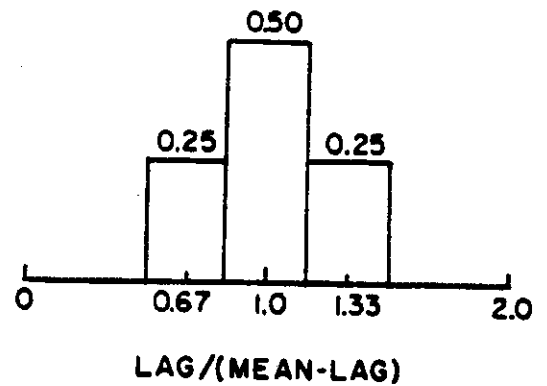


Figure 8. Frequency-Distribution for Lag

Low-loss fraction, \bar{Y}

The several reconstituted \bar{Y} parameters closely followed the relationship of Eq. (2). Consequently, there was only a small level of variation between the initial estimate of \bar{Y} from Eq. (2), and the optimized (reconstituted) value. The uncertainty in measured rain gauge precipitation depths and the noted \bar{Y} variations are modeled by the frequency-distribution for \bar{Y} as shown in Figure 9.

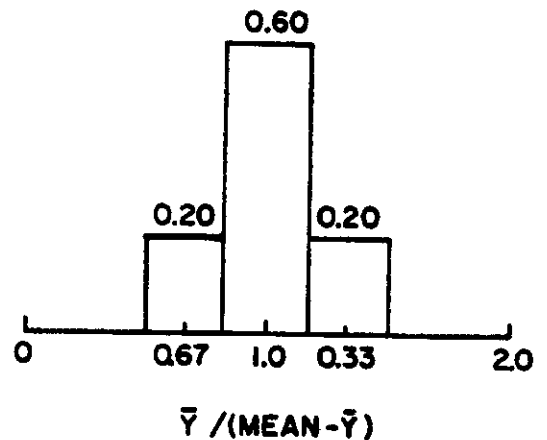


Figure 9. Frequency-Distribution for \bar{Y}

Evaluating UH model certainty

The UH model parameter frequency-distributions of Figures 3, 7, 8, 9 can be used to develop a universe of parameter sets, P_i , for evaluating the model output variance due to the variations in model parameters. From the figures it is seen that there are $(6) \times (8) \times (3) \times (3) = 432$ possible parameter sets as a combination of all parameter values, each with a probability of occurrence equal to the product of the individual parameter probability of occurrences.

It is recalled from a previous discussion, however, that this universe of parameter sets is an expansion of the true optimized parameter sets obtained from reconstitution studies of rainfall-runoff data. Furthermore, it is assumed in this study that the variations in parameters (from the expanded universe of parameter sets) is equal to the variance in model output due to the random selection of elements in the universe of optimized parameter sets, had a sufficient number of elements been available for study purposes.

2. TEST WATERSHEDS

Four watershed schematics are considered in this study in order to evaluate the effects of discretization. The "simple" model represents the entire catchment of 4500-acres as a single subarea. The remaining three "complex" models are based upon 3-, 9-, and 18- subareas linked together by channel routing links as shown in Figures 10, 11 and 12.

Each subarea has an associated runoff hydrograph representation given by Eq. (3). Subarea model parameters of Fm , \bar{Y} , X , and lag are chosen for the particular application problem considered.

Parameter identification

The usual procedure in using UH hydrologic models is to utilize regionalized model parameters of loss rates and the UH for subareas and to develop a link-node model schematic. The issue is whether the discretized (link-node) schematic is necessarily a "better" model than a simple single area model.

Assuming the variations in subarea parameters are identical to the variations in the regionalized parameters, the model uncertainty in estimated Q can be developed by varying all subarea parameters independently, resulting in a distribution of possible Q values. To evaluate modeling uncertainty, it is assumed in this study that all subarea selected design parameter estimates (P_d) are the mean values, and that the frequency-distributions of the parameters in the individual subareas are given by the simple 3-value distribution plots shown in Figure 13.

In all cases, the loss rate parameters are chosen for all 3 complex models so that the area-average of the subarea \bar{Y} and Fm mean values equals the simple model mean value for \bar{Y} and Fm . Additionally, the subarea X mean values (S -graph) are arbitrarily assigned and channel routing increments defined so that the complex model lag time equals the lag time of the single model.

It is noted that although the distribution of Q from each model is of interest, the focus of this study is on the $\text{Var}(Q)$ as developed from each model schematic.

3. THE EFFECTS OF DISCRETIZATION ON $\text{VAR}(Q)$

For the simple model, a Q is developed for each choice of parameter sets determined by the respective frequency-distributions. Consequently, using the frequency-distributions of Figure 13 indicates that $3^4 = 81$ runs are needed to exhaust the possible parameters sets. For each parameter set, P_i , the $\text{Prob}(P_i)$ equals the product of the individual parameter value frequencies. A frequency-distribution of Q values is developed by using all parameter sets.

In all cases, the rainfall input is a design storm pattern composed of nested, identical return-frequency rainfalls (without depth-area adjustment) such as described in HEC Training Document #15 (1982).

Figure 14 shows the Q frequency-distribution from the simple model for a 100-year storm. Shown in the figure are the estimated means and their standard deviations for an exhaustion analysis and three Monte Carlo studies. The plots indicate that a Monte Carlo method with a 1000 or 5000 number of simulations can achieve the same accuracy as the exhaustion model can. The use of Monte Carlo method is necessary due to the large number of elements composing the sample universe for the discretized models.

Discretization in parallel

Assuming the watershed can be subdivided in parallel subareas (Figure 15), and every subarea has identical parameters, it is seen that the $\text{Var}(Q)$ drops significantly. Other variations in this problem are to let the subarea sizes vary, include parameter nonhomogeneity, and increase the number of subareas. Table 3 summarizes the modeling results. From Table 3, $\text{Var}(Q)$ decreases as the number of subareas increase. Also parameter nonhomogeneity did not significantly impact the $\text{Var}(Q)$.

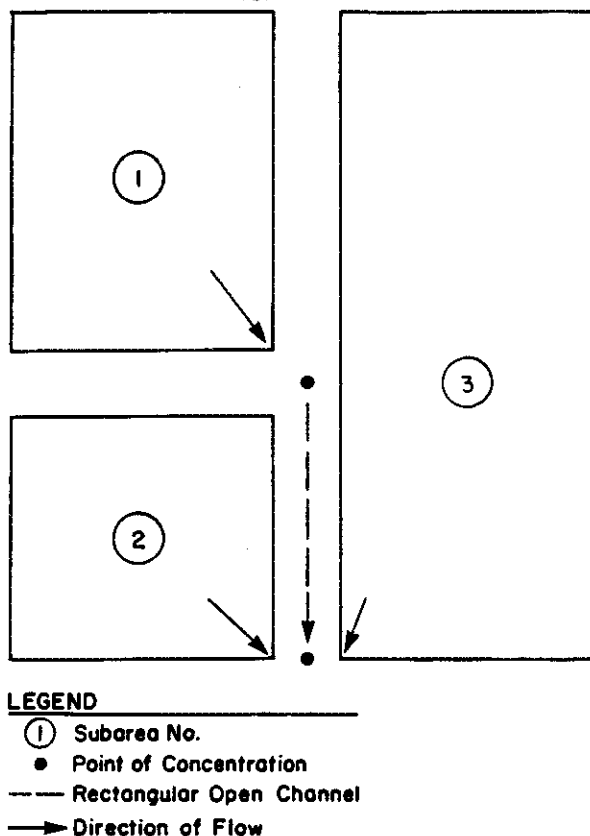


Figure 10. Test Watershed Schematic of 3-Subarea Link-Node Model

Table 3. Discretization in Parallel Model Results

| Test No. | Subarea No. | Subarea (acres) | Lag (hrs) | Fm | Y | X | $Q^{(1)}$ | $\sigma^{(2)}$ |
|----------|-------------|-----------------|-----------|-------|-------|-------|-----------|----------------|
| 1 | 1 | 4500 | 1.0 | 0.20 | 0.25 | 0.70 | 4826 | 784 |
| 2 | 1 | 2250 | 1.0 | 0.20 | 0.25 | 0.70 | 4724 | 541 |
| | 2 | 2250 | 1.0 | 0.20 | 0.25 | 0.70 | | |
| 3 | 1 | 3000 | 1.0 | 0.20 | 0.25 | 0.70 | 4735 | 575 |
| | 2 | 1500 | 1.0 | 0.20 | 0.25 | 0.70 | | |
| 4 | 1 | 3000 | 1.0 | 0.225 | 0.275 | 0.675 | 5410 | 707 |
| | 2 | 1500 | 0.45 | 0.150 | 0.200 | 0.750 | | |
| 5 | 1-6 | 750 | 1.0 | 0.20 | 0.25 | 0.70 | 4669 | 302 |

Notes:

¹ Q is the mean peak flow rate (Q)

² σ is the standard deviation of Q

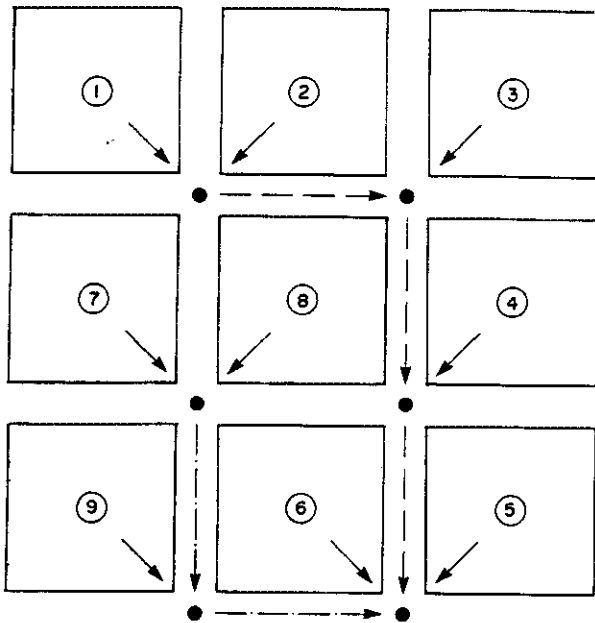
³ 5000-run Monte Carlo simulations used

⁴ 100-year design storm used for all studies

However for homogeneous subareas of equal size, the $\text{Var}(Q)$ is empirically estimated by

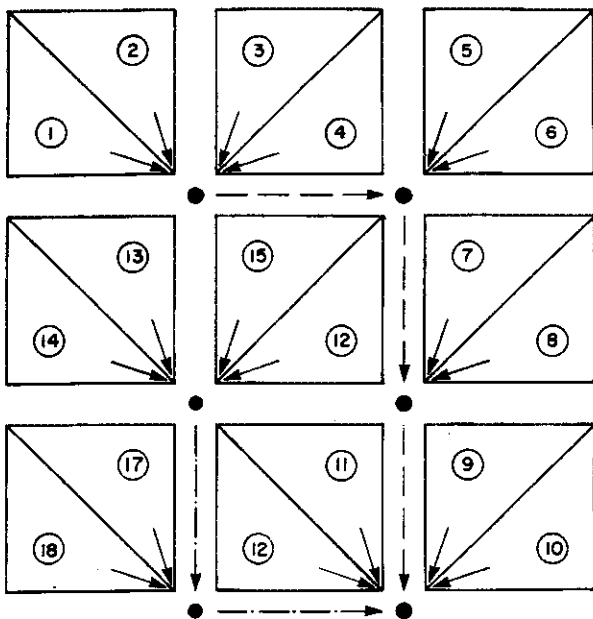
$$\text{Var}_m(Q) = \frac{1}{m} \text{Var}_1(Q) \quad (5)$$

where m is the number of subareas, and $\text{Var}_1(Q)$ is the $\text{Var}(Q)$ for the single area model. Hence from Eq. (5), $\text{Var}_m(Q) \rightarrow 0$ as $m \rightarrow \infty$.



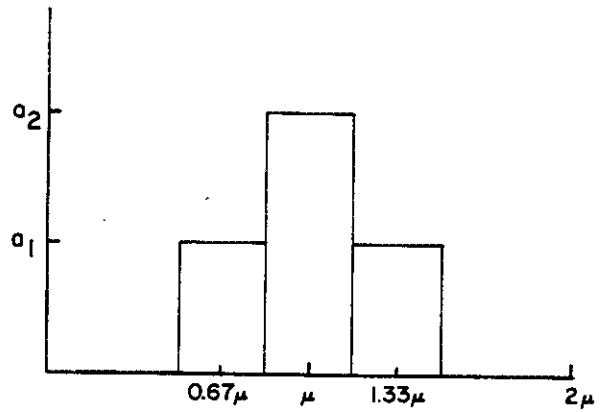
LEGEND
 ① Subarea No.
 ● Point of Concentration
 - - - Rectangular Open Channel #1
 - - - Rectangular Open Channel #2
 → Direction of Flow

Figure 11. Test Watershed Schematic of 9-Subarea Link-Node Model



LEGEND
 ① Subarea No.
 ● Point of Concentration
 - - - Rectangular Open Channel #1
 - - - Rectangular Open Channel #2
 → Direction of Flow

Figure 12. Test Watershed Schematic of 18-Subarea Link-Node Model



LEGEND
 μ Assumed Parameter Mean Value
 a_1 { .25 for Lag
 .20 Other Parameters
 a_2 { .50 for Lag
 .60 Other Parameters

Figure 13. Assumed Frequency Distribution Plot for selected Watershed Parameters

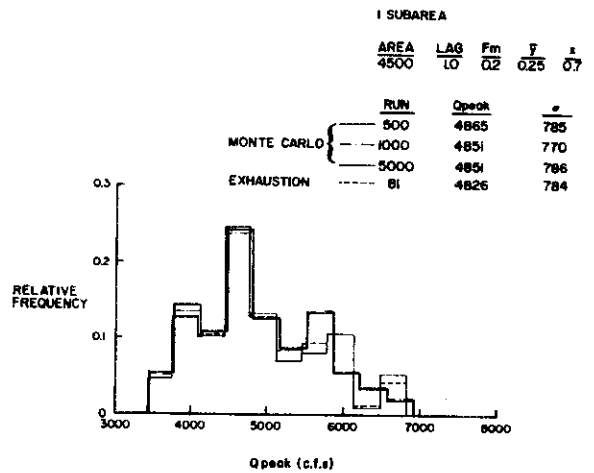
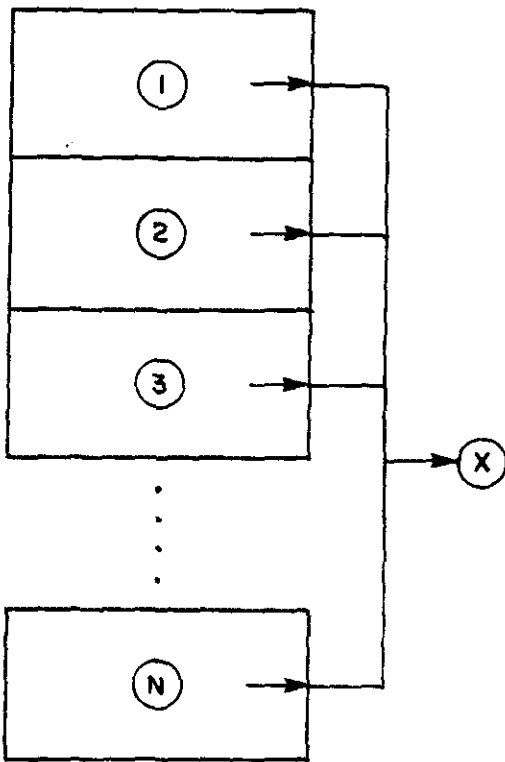


Figure 14. Single Area Model Q Frequency-Distribution (100-year Storm)



LEGEND

- ① Subarea No.
- Flow Direction
- ⊗ Point of Concentration

Figure 15. Schematic for N-Parallel Subareas Model

Discretization in series

Subdivision of the catchment in series and linking the subareas together by channel routing is the general modeling situation. Using convex channel routing, which operates on a single reproducible parameter C , and assuming a frequency-distribution as shown in Figure 13, an analysis of the $\text{Var}(Q)$ can be prepared.

Figure 16 shows the two subareas schematic and channel information. Both a steep (fast flow) and mild (slow flow) channel are considered. Also shown are $\text{Var}(Q)$ results with and without variations in the convex routing parameter C . Table 4 summarizes the $\text{Var}(Q)$ modeling results for a variety of conditions, using the schematics shown in Figures 10, 11, 12, and 16.

Magnitude of storm

Another variant of the above analysis is to consider a 10-year design storm rather than a 100-year design storm. As expected, the mean Q values decreased from the Table 4 values, but the $\text{Var}(Q)$ decreased only slightly. However, it was still true that $\text{Var}(Q)$ decreased as the number of subareas increased.

4. IS DISCRETIZATION BETTER?

In order to better explain the interplay between the several previous discussions; consider the following thought problem: Let the watershed be essentially homogeneous,

nearly free-draining, with a stream gauge and an off-site rain gauge. (The rain gauge is assumed off-site to emphasize a point.)

Suppose a set of 100 severe storms occur such that the measured rainfall, $p^i(t)$, and measured effective rainfalls, $e_g^i(t)$, at the rain gauge (which has soil similar to the watershed) is known, for $i = 1, 2, \dots, 100$. Furthermore, suppose each $p^i(t)$ and $e_g^i(t)$ is identical and equal to a single pattern, $p(t)$, $e_g(t)$, respectively, for each storm, while the rainfalls over the catchment differ for each storm. Therefore even though each $p^i(t)$ and $e_g^i(t)$ is identical, the runoff hydrograph $Q^i(t)$ is different for every i . Let Q_p^i be the peak flow rate for each $Q^i(t)$.

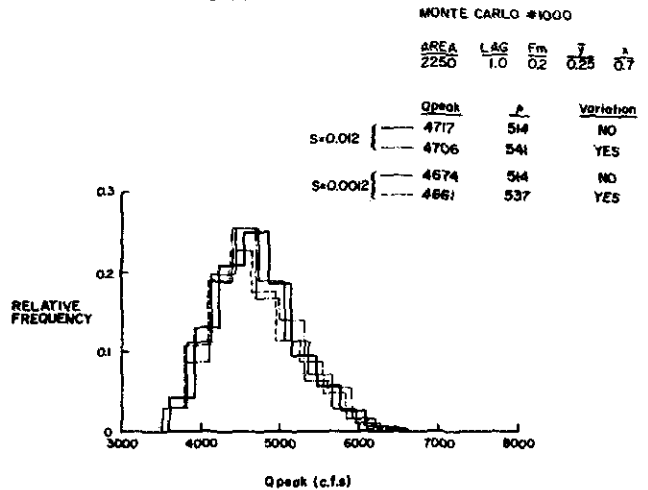


Figure 16. Two Subareas Model Q Frequency-Distribution (100-year Storm)

Then from a frequency-distribution plot of the Q_p^i , the $\text{Var}(Q_p)$ can be computed as correlated to the available rainfall data (at the rain gauge site), and for the sample set of $\{Q_p^i\}$.

By calibrating the simple model, $q_s(t)$, to each $Q^i(t)$, a set of optimized parameters P_i are developed for each $i = 1, 2, \dots, 100$. Since the rainfall distribution at the rain gauge, $p^i(t) = p(t)$, is fixed, the $\text{Var}(Q)$ from $q_s(t)$ due to the variation in optimized parameter sets, $\{P_i\}$, approximately equals the $\text{Var}(Q_p)$.

In contrast, when discretizing the catchment, $\text{Var}(Q)$ produced by the discretized model essentially decreases significantly with the level of discretization, when mostly parallel routing is used, when using the parameters developed from the $q_s(t)$ calibration. Thus the complex model output (of peak flow rate, Q) does not show the true natural variance between the rain gauge and stream gauge correlations.

However with a stream gauge in each subarea, each subarea's model parameters can be optimized for each storm such that the complex model produced $\text{Var}(Q)$ equals the simple model produced $\text{var}(Q)$ which equals the true $\text{Var}(Q)$ with respect to the available (single) rain gauge.

Therefore, if a criteria for model comparison is that the model replicates the $\text{Var}(Q_p)$ with respect to the available rain gauge data, then the simple model does this better than the highly discretized model.

Table 4. Discretization in Series Modeling Results

| Test No. | Subarea No. | Area (acres) | Lag (hrs) | Fm | Y | X | flow ⁽¹⁾ | C ⁽²⁾ | Q ⁽³⁾ | σ ⁽⁴⁾ |
|-------------------|-------------|------------------------|-----------|-------|------|-------|---------------------|------------------|------------------|-------------------------|
| 1 | 1.2 | 2250 | 1.0 | 0.20 | 0.25 | 0.70 | fast | no | 4717 | 514 |
| 2 | 1.2 | 2250 | 1.0 | 0.20 | 0.25 | 0.70 | fast | yes | 4706 | 514 |
| 3 | 1.2 | 2250 | 1.0 | 0.20 | 0.25 | 0.70 | slow | no | 4674 | 514 |
| 4 | 1.2 | 2250 | 1.0 | 0.20 | 0.25 | 0.70 | slow | yes | 4661 | 537 |
| 5 | 1 | 2250 | 0.83 | 0.20 | 0.25 | 0.70 | slow | no | 4977 | 547 |
| | 2 | 2250 | 1.0 | 0.20 | 0.25 | 0.70 | slow | yes | 4962 | 572 |
| 6 ⁽⁵⁾ | 1 | 1500 | 0.85 | 0.075 | 0.30 | 0.475 | | | | |
| | 2 | 750 | 1.0 | 0.15 | 0.15 | 0.85 | | | | |
| | 3 | 2250 | 1.0 | 0.30 | 0.25 | 0.80 | fast | no | 4977 | 528 |
| 7 | | | | | | | fast | yes | 4963 | 550 |
| 8 | | | | | | | slow | no | 5009 | 529 |
| 9 | | | | | | | slow | yes | 4988 | 549 |
| 10 ⁽⁶⁾ | 1 | 400 | .85 | 0.20 | 0.20 | 0.65 | | | | |
| | 2 | 600 | .85 | 0.10 | 0.15 | 0.80 | | | | |
| | 3 | 550 | .90 | 0.20 | 0.20 | 0.75 | | | | |
| | 4 | 350 | .95 | 0.30 | 0.35 | 0.70 | | | | |
| | 5 | 450 | 1.0 | 0.20 | 0.30 | 0.85 | | | | |
| | 6 | 650 | 1.0 | 0.30 | 0.35 | 0.70 | | | | |
| | 7 | 500 | .80 | 0.20 | 0.30 | 0.60 | | | | |
| | 8 | 360 | .80 | 0.30 | 0.25 | 0.65 | | | | |
| | 9 | 640 | .90 | 0.20 | 0.25 | 0.60 | slow | no | 4887 | 290 |
| 11 | | | | | | | slow | yes | 4992 | 294 |
| 12 ⁽⁷⁾ | (1-18) | ---- homogeneous ----- | | | | | slow | no | 5961 | 274 |
| 13 | | | | | | | slow | yes | 5945 | 277 |

Notes:

- ¹ flow: "fast" = steep channel, "slow" = mild channel
- ² C = convex routing C parameter variation
- ³ Q = mean Q
- ⁴ σ = standard deviation in Q
- ⁵ 3 = subarea schematic (Figure 10)
- ⁶ 9 = subarea schematic (Figure 11)
- ⁷ 18 = subarea schematic (Figure 12)
- ⁸ 100-year design storm used in all studies
- ⁹ 5000-run Monte Carlo simulations used

REFERENCES

- 1 Scully, D. and Bender, D., Separation of Rainfall Excess from Total Rainfall, *Water Resources Research*, 1969, 5, 4, August
- 2 Kibler, D., (Ed.), Urban Storm Water Hydrology, Water Resources Monograph 7, American Geophysical Union, Washington, D.C., 1982
- 3 McCuen, R. and Bondelid, T., Estimating Unit Hydrograph Peak Rate Factors, *Journal of Irrigation and Drainage Engineering*, 1983, 109, 2, June
- 4 Chow, V. and Kulandaiswamy, V., The IUH of General Hydrologic Systems Model, *Journal of Hydraulics Division*, Proceedings of the American Society of Civil Engineers, No. HY7, July, 1982, 108
- 5 Mays, L. and Coles, L., Optimization of Unit Hydrograph Determination, *Journal of the Hydraulics Division*, 1980, 106, No. HY1, January